Origin of volatiles in the Main Belt

Olivier Mousis, Yann Alibert, D. Hestroffer, Ulysse Marboeuf, Christophe Dumas, Benoit Carry, Jonathan Horner, Franck Selsis

Mon. Not. R. Astron. Soc. **383,** 1269–1280 (2008) doi:10.1111/j.1365-2966.2007.12653.x

Origin of volatiles in the main belt

O. Mousis,[1⋆] Y. Alibert,[1,2] D. Hestroffer,[3] U. Marboeuf,[1] C. Dumas,[4] B. Carry,[4] J. Horner[5] and F. Selsis[6,7]

[1]*Institut UTINAM, CNRS-UMR 6213, Observatoire de Besançon, BP 1615, 25010 Besançon Cedex, France*
[2]*Physikalisches Institut, University of Bern, Sidlerstrasse 5, CH-3012 Bern, Switzerland*
[3]*IMCCE, CNRS-UMR 8028, Observatoire de Paris, 77 Av. Denfert Rochereau, 75014 Paris, France*
[4]*ESO, Alonso de Cordova 3107, Vitacura, Casilla 19001, Santiago 19 Chile*
[5]*Astronomy Group, Open University, Walton Hall, Milton Keynes MK7 6AA*
[6]*C.R.A.L, Ecole normale supérieure, 46 allée d'Italie, 69007 Lyon, France*
[7]*Laboratoire d'Astrophysique de Bordeaux, CNRS, Université Bordeaux 1, BP 89, F-33270 Floirac, France*

Accepted 2007 October 24. Received 2007 October 4; in original form 2007 May 29

ABSTRACT

We propose a scenario for the formation of the main belt in which asteroids incorporated icy particles formed in the outer solar nebula. We calculate the composition of icy planetesimals formed beyond a heliocentric distance of 5 au in the nebula by assuming that the abundances of all elements, in particular that of oxygen, are solar. As a result, we show that ices formed in the outer solar nebula are composed of a mix of clathrate hydrates, hydrates formed above 50 K and pure condensates produced at lower temperatures. We then consider the inward migration of solids initially produced in the outer solar nebula and show that a significant fraction may have drifted to the current position of the main belt without encountering temperature and pressure conditions high enough to vaporize the ices they contain. We propose that, through the detection and identification of initially buried ices revealed by recent impacts on the surfaces of asteroids, it could be possible to infer the thermodynamic conditions that were present within the solar nebula during the accretion of these bodies, and during the inward migration of icy planetesimals. We also investigate the potential influence that the incorporation of ices in asteroids may have on their porosities and densities. In particular, we show how the presence of ices reduces the value of the bulk density of a given body, and consequently modifies its macroporosity from that which would be expected from a given taxonomic type.

Key words: minor planets, asteroids – Solar system: formation.

1 INTRODUCTION

In recent years, some objects within the main belt of asteroids have been found to display cometary characteristics (Hsieh & Jewitt 2006). Objects such as 133P/Elst-Pizarro, P/2005 U1 and 118401 (1999 RE_{70}) occupy orbits that are entirely decoupled from Jupiter within the main belt, and are probably bodies that have undergone a recent collision, revealing previously buried volatile material and leading to the observed dusty outgassing. In addition, present-day surface water ice and possible water sublimation have been reported on Ceres (Lebofsky et al. 1981; A'Hearn & Feldman 1992; Vernazza et al. 2005). This is consistent with recent *Hubble Space Telescope* (*HST*) observations which suggest that Ceres' shape is the result of the dwarf planet consisting of a rocky core surrounded by an ice-rich mantle (Thomas et al. 2005) – an idea in agreement with several thermal evolution scenarios (McCord & Sotin 2005) that suggest that the ice content of the asteroid is between 17 and 27 per cent, by mass. These observations are supported by the evidence of hydrated minerals in meteorites which provide samples of rock from asteroids in the main belt. Most of these minerals formed as a result of water ice accreting with the chondritic meteorite parent bodies, melting and driving aqueous alteration reactions (Clayton & Mayeda 1996; Jewitt et al. 2007).

It seems likely, then, that some objects in the asteroid belt have incorporated significant amounts of water ice (and possibly other volatiles) during their formation in the early stages of the Solar system. These bodies would have incorporated icy particles[1] coming from the outer nebula that survived their inward drift due to gas drag through the disc (Mousis & Alibert 2005, hereafter MA05). The volatile fraction incorporated in this manner could vary depending on the inward flux of icy planetesimals from the external region and

⋆E-mail: olivier.mousis@obs-besancon.fr

[1] By icy particles is meant planetesimals composed of a mix of ices and rocks.

the heliocentric location of the asteroid, together with the density of the protosolar nebula. Given that the current asteroid belt lies closer to the Sun than the 'snowline', postulated to lie at around 5 au in the solar nebula, these results are a little unexpected. In this context, understanding how volatiles were incorporated into the asteroids is therefore important, not only for the study of the asteroids themselves, but also for our understanding of the processes by which the Solar system came into being.

To this end, MA05 studied the possibility of determining the nature and composition of the ices which were incorporated into Ceres. They used a time-dependent model of the solar nebula and showed that icy particles of sizes between 0.1 and 10 m could drift from heliocentric distances greater than 5 au to the present location of Ceres without encountering temperatures or pressures high enough to vaporise the ices within. The authors then suggested that ices produced in the outer solar nebula were transported inwards to become incorporated in the solids which accreted to form Ceres.

The present work aims to improve upon the calculation detailed in MA05, along with expanding the results to involve the entire asteroid belt, rather than just its largest member. In particular, MA05 postulated that all volatiles, except CO_2,[2] were trapped by water in the form of hydrates or clathrate hydrates in the outer solar nebula. This assumption was supported by the work of Hersant, Gautier & Huré (2001) who estimated that Jupiter was formed at temperatures higher than ∼40–50 K. The accretion of ices in the form of hydrates and clathrate hydrates was thus required during the formation of the planet in order to explain the volatile enrichments observed in its atmosphere[3] (Gautier et al. 2001b,a). Indeed, since these ices are usually formed at temperatures higher than that reached by the nebula at the time of Jupiter's completion, as defined by Hersant et al. (2001), they can be incorporated in the planetesimals accreted by the giant planet during its growth. However, the amount of water that would be required in the nebula to trap all these volatiles as hydrates and clathrate hydrates exceeds that derived from the solar oxygen abundance. Therefore, MA05 made the ad hoc hypothesis that oxygen was 'oversolar' in the gas phase in order to provide enough available water in the solar nebula.[4] Additionally, Hersant et al. (2001) only used an evolutionary solar nebula model to derive the disc's temperature at the time when the mass of Jupiter's feeding zone was equal to that of the gas in its current envelope. They thus neglected many important effects such as the influence of protoplanet formation on the structure of the disc (e.g. fig. 2 of Alibert, Mordasini & Benz 2004). However, recent giant planet core-accretion formation models that include migration, disc evolution, such as that proposed by Alibert et al. (2004), have shown that the disc's temperature can be as low as ∼10–20 K at the end of Jovian formation. This implies that Jupiter itself can accrete ices during its formation that were produced at temperatures lower than those required for clathration. As a result, no extra water is required in the nebula to allow all the volatile species to be trapped in clathrate hydrates, and the oversolar oxygen abundance condition in the nebula can be relaxed.

In Section 2, we calculate the composition of ices produced in the outer solar nebula under the assumption that the abundances of all elements, in particular that of oxygen, are solar. In Section 3, we consider the inward migration of particles produced at various locations in the nebula, and at different times. This allows us to examine whether some planetesimals formed in the outer solar nebula may have drifted to the current position of the main belt without encountering temperature and pressure conditions high enough to vaporize the ices they contain. In Section 4, we examine the uncertainties in the determination of the physical properties of asteroids. We also investigate the potential influence that the incorporation of ices in these objects may have on their porosities and densities. Section 5 is devoted to summary and discussion.

2 COMPOSITION OF ICY PLANETESIMALS FORMED IN THE OUTER SOLAR NEBULA

2.1 Initial gas-phase conditions in the nebula

In this section, we aim to estimate the composition of icy particles produced in the region of giant planet formation, prior to the dissipation of the nebula, which then migrated into the forming main belt. The calculations have been carried out in a manner consistent with the formation of Jupiter with a realistic primordial volatile composition. This implies that the icy planetesimals that drifted inwards to the formation zone of the asteroids shared the same composition as those accreted by proto-Jupiter.

We then assume that the gas-phase abundances of elements are solar (e.g. Table 1) and that O, C and N exist only in the form of H_2O, CO_2, CO, CH_4, N_2 and NH_3. S is only present as H_2S and other refractory sulphur components (Pasek et al. 2005). The gas-phase molecular ratios in the solar nebula are presumed to derive directly from that in interstellar ices (Mousis, Gautier & Bockelée-Morvan 2002) and, in some cases, from the consideration of catalytic effects that might affect these ratios in the nebula. Thus, although the CO:CH_4 ratio is typically around 10:1 in the interstellar medium (ISM) (Allamandola et al. 1999), this can be revised down in the solar nebula gas phase since some additional CH_4 may be introduced through conversions of both CO and CO_2, as a result of the presence of catalytically active regions in the disc (Kress & Tielens 2001; Sekine et al. 2005). We, therefore, adopt CO:CH_4 = 1:1 in the vapour phase of the nebula. Moreover, CO_2 should initially be present in the gas phase of the nebula, with CO_2:CO = 1:1–4:1, a range of values that covers the ISM measurements (Gibb et al. 2004). The value of the N_2:NH_3 ratio is quite uncertain, although current chemical models of the ISM predict that molecular nitrogen should be much

Table 1. Gas-phase abundances (molar mixing ratio with respect to H_2) of major species in the solar nebula from Lodders (2003) with CO_2:CO:CH_4 = 1:1:1 and N_2:NH_3 = 1:1.

Species X	X/H_2	Species X	X/H_2
O	1.16×10^{-3}	N_2	5.33×10^{-5}
C	5.82×10^{-4}	NH_3	5.33×10^{-5}
N	1.60×10^{-4}	S	3.66×10^{-5}
H_2O	5.78×10^{-4}	Ar	8.43×10^{-6}
CO_2	1.94×10^{-4}	Kr	4.54×10^{-9}
CO	1.94×10^{-4}	Xe	4.44×10^{-10}
CH_4	1.94×10^{-4}		

[2] CO_2 is the only major volatile species which does not form a clathrate hydrate in the solar nebula because it condenses as a pure ice prior to being trapped by water.

[3] The abundances of volatile species in Jupiter's atmosphere have been measured using the mass spectrometer on board the *Galileo* probe. These measurements reveal that the giant planet's atmosphere is enriched by a factor of ∼3 in Ar, Kr, Xe, C, N and S compared to the solar abundances (Owen et al. 1999).

[4] The oxygen abundance required for to allow the trapping of all volatile species in the form of hydrates or clathrate hydrates is ∼1.9 times the solar abundance, with CO_2:CO:CH_4 = 1:1:1 and N_2:NH_3 = 1:1 (the nominal nebula gas phase ratios used in this work).

more abundant than ammonia (Irvine & Knacke 1989). On the other hand, the N_2:NH_3 ratio may have been much lower in the solar nebula since the conversion of N_2 into NH_3 can be accelerated by the catalytic effect of local Fe grains (Lewis & Prinn 1980; Fegley 2000). In all our following calculations, we consider N_2:NH_3 = 1:1 as the nominal ratio for these two molecules in the nebula gas phase.

2.2 Formation sequence of the different ices in the outer nebula

As a result of the adoption of a solar gas-phase oxygen abundance, we show here that ices formed at distances greater than 5 au in the cooling solar nebula are a mix of clathrate hydrates and hydrates formed above 50 K, and pure condensates primarily produced at lower temperatures (but still greater than ∼20 K). We note that this hypothesis is supported by the recent work of Mousis & Marboeuf (2006), who showed that the abundances of volatiles observed in the envelopes of Jupiter and Saturn could be reproduced by using a solar abundance for all elements in the solar nebula, and that the calculated amount of heavy elements remains in agreement with internal structure models. The clathration and hydratation processes result from the presence of available crystalline water ice at the time of volatile trapping in the solar nebula. This statement seems justified when one considers that current scenarios of the formation of the solar nebula suggest that most ices falling from the pre-solar cloud on to the disc were vaporized upon entering the early nebula. Following Chick & Cassen (1997), H_2O ice is initially vaporized at locations in the inner 30 au of the solar nebula. With time, the decrease of temperature and pressure led to conditions which allowed the water to recondense, forming microscopic crystalline ices (Kouchi et al. 1994; Mousis et al. 2000). Once formed, the different ices agglomerated and were incorporated into the growing and drifting particles.

The process by which volatiles are trapped, illustrated in Fig. 1, is calculated using the stability curves of hydrates, clathrate hydrates and pure condensates, and the tracks detailing the evolution of temperature and pressure at heliocentric distances of 5, 15 and 20 au within the solar nebula. These evolutionary tracks are derived from the α-turbulent accretion disc model described in next section. The stability curves of hydrates and clathrate hydrates derive from Lunine & Stevenson (1985) compilation of laboratory data, from which data is available at relatively low temperature and pressure. Their equations, given by Hersant, Gautier & Lunine (2004), are of the form $\ln P = A/T + B$, where P and T are the partial pressure (bars) and the temperature (K) of the considered species, respectively. Table 2 shows the values of constants A and B determined by Hersant et al. (2004) from their fits to laboratory measurements. On the other hand, the stability curves of pure condensates used in our calculations derive from the compilation of laboratory data given in the CRC Handbook of Chemistry and Physics (Lide 2002). Their equations are of the form $\log P = A/T + B$, where P and T have the same units as mentioned above. Table 3 also gives the constants A and B as determined by our own fits to laboratory measurements. The cooling curve intercepts the stability curves of the different ices at some given temperature, pressure and surface density conditions (see Table 4). For each ice considered, the domain of stability is the region located below its corresponding stability curve. The clathration process stops when no more crystalline water ice is available to trap the volatile species. For example, if one assumes CO_2:CO:CH_4 = 1:1:1 and N_2:NH_3 = 1:1 in the gas phase, then the NH_3 and H_2S are entirely trapped by the water, as hydrates of NH_3 and clathrate hydrates of H_2S, while only approximately half of the CH_4 is trapped

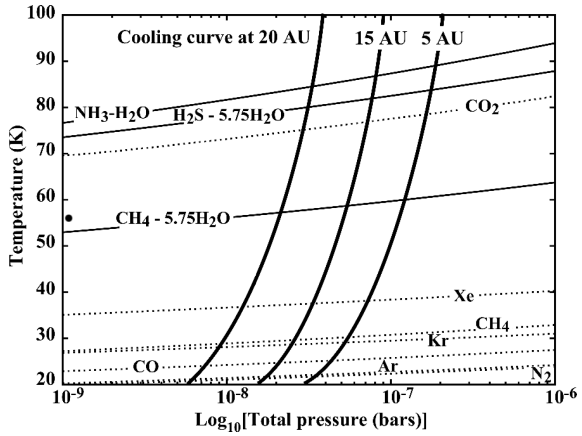

Figure 1. Stability curves for hydrates, clathrate hydrates (solid lines) and pure condensates (dotted lines), together with evolutionary tracks for the nominal protoplanetary disc model at heliocentric distances of 5, 15 and 20 au. These evolutionary tracks correspond to the thermodynamic pathway followed by the disc during its cooling at the considered distances to the Sun (the evolution of the disc proceeds from high to low temperatures). The abundances of elements are solar, with CO_2:CO:CH_4 = 1:1:1 and N_2:NH_3 = 1:1 in the vapour phase. Species remain in the vapour phase as long as they stay in the domains located above the curves of stability. The label $-5.75H_2O$ designates the clathrate hydrate of species X and NH_3–H_2O corresponds to ammonia hydrate.

Table 2. Parameters of the stability curves of the considered clathrate hydrates (reproduced from Hersant et al. 2004). Their equations are of the form $\ln P = A/T + B$, where P and T are the partial pressure (bars) and the temperature (K) of the considered species, respectively. A is in K and B is dimensionless.

Species	A	B
CH_4	−2161.81	11.1249
CO	−1685.54	10.9946
N_2	−1677.62	11.1919
NH_3	−2878.23	8.00205
H_2S	−3111.02	11.3801
Ar	−1481.78	9.95523
Kr	−1987.5	9.99046
Xe	−2899.18	11.0354

Table 3. Parameters of the stability curves of the considered pure condensates. Their equations are of the form $\log P = A/T + B$, where P and T are the partial pressure (bars) and the temperature (K) of the considered species, respectively. A is in K and B is dimensionless.

Species	A	B
CH_4	−475.61	4.2831
CO	−411.24	5.2426
CO_2	−1365.9	7.0248
N_2	−360.07	4.7459
NH_3	−1565.0	6.7883
H_2S	−1153.70	5.5007
Ar	−369.90	4.1862
Kr	−603.46	5.1060
Xe	−819.28	4.9881

Table 4. Temperature T (K), total gas pressure P (bars) and surface density Σ (g cm^{-2}) conditions at which different ices form in the solar nebula at heliocentric distance of 5 au. The gas-phase conditions considered here are CO_2:CO:CH_4 = 1:1:1 and N_2:NH_3 = 1:1.

Ices	T (K)	P (bar)	Σ (g cm^{-2})
H_2O	157.5	3.4×10^{-7}	677.4
NH_3–H_2O	89.1	1.9×10^{-7}	498.0
H_2S–5.75H_2O	84.0	1.8×10^{-7}	482.6
CO_2	78.0	1.6×10^{-7}	463.8
CH_4–5.75H_2O	60.9	1.3×10^{-7}	404.3
Xe	38.2	7.6×10^{-8}	301.1
CH_4	31.3	6.0×10^{-8}	259.1
Kr	29.2	5.4×10^{-8}	244.4
CO	25.3	4.5×10^{-8}	213.9
Ar	22.2	3.6×10^{-8}	185.6
N_2	21.8	3.5×10^{-8}	181.7

as a clathrate hydrate in the solar nebula. The remaining CH_4, as well as Xe, Kr, CO, Ar and N_2, whose clathration processes normally occur at higher temperatures, remain in the vapour phase until the solar nebula cools enough to allow the formation of pure condensates (roughly between 20 and 30 K in the gas-phase conditions assumed for the solar nebula; see Fig. 1). Note that, during the cooling of the solar nebula, CO_2 is the only species that crystallizes as a pure condensate prior to being trapped by water to form a clathrate hydrate. Hence, we assume here that solid CO_2 is the only existing condensed form of CO_2 in these environments.

2.3 Composition of icy planetesimals

Using the trapping/formation conditions of the different ices calculated at a given heliocentric distance in the outer nebula (e.g. Table 4), and knowing their gas-phase abundances, one can estimate their mass ratios with respect to H_2O in the accreting planetesimals. Indeed, the volatile, i, to water mass ratio in these planetesimals is determined by the relation given by Mousis & Gautier (2004):

$$m_i = \frac{X_i}{X_{H_2O}} \frac{\Sigma(R; T_i, P_i)}{\Sigma(R; T_{H_2O}, P_{H_2O})}, \quad (1)$$

where X_i and X_{H_2O} are the mass mixing ratios of the volatile i and H_2O with respect to H_2 in the solar nebula, respectively. $\Sigma(R; T_i, P_i)$ and $\Sigma(R; T_{H_2O}, P_{H_2O})$ are the surface density of the nebula at a distance R from the Sun at the epoch of hydratation or clathration of the species i, and at the epoch of condensation of water, respectively. From m_i, it is possible to determine the mass fraction of species i with respect to all the other volatile species taking part to the formation of an icy solid:

$$M_i = \frac{m_i}{\sum_{j=1,n} m_j}, \quad (2)$$

with $\sum_{i=1,n} M_i = 1$.

It is important to mention that, after having performed calculations using a wide range of values from 10^{-3} to 10^{-1} for the viscosity parameter α of our turbulent model, we found that the volatile trapping conditions (temperature and pressure) remain almost constant at a given heliocentric distance in the solar nebula, whatever the adopted value of this parameter. In addition, Alibert, Mousis & Benz (2005a) demonstrated that the composition of icy planetesimals remains similar whatever their formation distance within the same disc, as long as a homogeneous gas phase is postulated within the nebula. These statements imply that, whatever the input parameters adopted when modelling the disc, and regardless of the formation location considered for icy planetesimals at distances beyond 5 au, their composition (in wt per cent) remains almost constant, provided that the gas-phase abundances are homogeneous in the nebula.

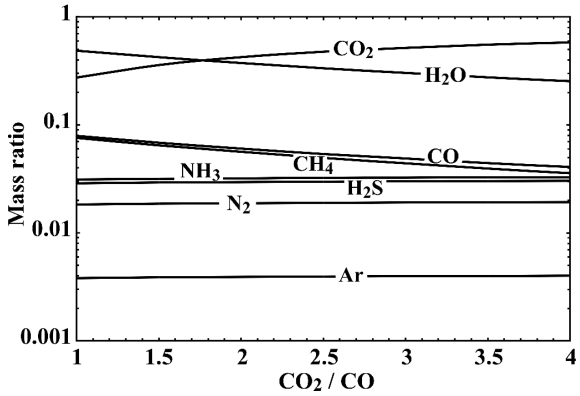

Figure 2. Plot showing the composition of the ices (wt per cent) incorporated in planetesimals produced in the solar nebula as a function of the adopted CO_2:CO ratio in the initial vapour phase. The composition is expressed as a mass ratio (mass of ice i to the global mass of ices). The abundances of the considered elements are solar with CO:CH_4 = 1:1 and N_2:NH_3 = 1:1 in the vapour phase. Note that the mass fractions of Kr and Xe are too low to be represented given the scale adopted in the figure.

Fig. 2 shows the variation of the composition of icy planetesimals formed in the outer solar nebula as a function of the CO_2:CO ratio (shown for values between 1:1 and 4:1), with CO:CH_4 = 1:1 and N_2:NH_3 = 1:1 in the gas phase. The composition of ices given in this figure is then valid for solids formed at any distance within the outer solar nebula, provided that the gas phase is homogeneous and the disc is initially warm enough at that location to vaporize the ices falling in from the ISM. It can be seen that water remains the most abundant ice in mass, provided that the CO_2:CO gas-phase ratio in the nebula is between 1 and ∼1.7. Interestingly enough, whatever the assumed CO_2:CO ratio, CO_2 remains the main carbon species trapped within planetesimals. We also note that the relative amounts of H_2O and of other carbon species decrease as the CO_2:CO ratio increases. In contrast, the mass fractions of NH_3, N_2, H_2S and of the noble gases are only weakly influenced by the variation of the CO_2:CO gas-phase ratio. Table 5 gives the mass ratios of the ices for the two extreme cases CO_2:CO = 1:1 and 4:1.

3 DELIVERY OF ICY PARTICLES TO THE MAIN BELT

Particles in protoplanetary discs undergo orbital decay due to the effects of gas drag (Weidenschilling 1977). The efficiency of this process is particularly dependent on the gas density inside the disc, and on the size and density of the particles. Cyr, Sears & Lunine (1998) showed that icy particles produced in the outer Solar system may have been incorporated in bodies formed in the inner regions. Indeed, taking into account gas drag, sedimentation and sublimation, these authors calculated that particles originating from ∼5 au may migrate to heliocentric distances of the order of 3 au due to gas drag, before subliming as a consequence of the higher temperature and pressure domains encountered in the inner regions. However, it is

Table 5. Ratio of the mass of ice i to the global mass of ices (wt per cent) in planetesimals formed in the outer solar nebula, calculated for CO_2:CO = 1:1 and 4:1 in the vapour phase. Both ratios are calculated with CO:CH_4 = 1:1 and N_2:NH_3 = 1:1 in the gas phase of the nebula.

Species	CO_2:CO = 1:1	CO_2:CO = 4:1
H_2O	48.8	25.5
CO_2	27.5	58.4
CO	7.9	4.2
CH_4	7.6	3.7
NH_3	∼3.3	
H_2S	∼2.9	
N_2	∼1.9	
Ar	≪ 0.1	
Kr	≪ 0.1	
Xe	≪ 0.1	

important to note that Supulver & Lin (2000), Cuzzi et al. (2005) and Ciesla & Cuzzi (2006) were unable to reproduce these results. More recently, MA05 examined the effect of gas drag on the migration of icy particles using a time-dependent model of the solar nebula.[5] They demonstrated that, after the Solar system has experienced a few Myr of cooling, it is possible for icy particles from the outer Solar system to drift inward to the present location of Ceres (∼2.7 au). In such an evolved system, because the snowline has already passed through the main belt, the volatiles contained in the icy particles can avoid sublimation during their migration.

In this paper, we extend the calculations originally performed by MA05, in order to take into account the possibility of volatile capture directly in the form of pure ice, in case there is too little water to trap all volatiles as hydrates and clathrate hydrates. Moreover, for the sake of consistency, we use the disc model that allows the formation of Jupiter and Saturn, leading to planets with internal structures consistent with observations (see Alibert et al. 2005b).

The numerical procedure used to calculate the structure and evolution of the disc are entirely detailed in Alibert et al. (2005c), and in this work we only give the main points. More details can be found in the afore-mentioned paper. The surface density Σ in the disc is calculated by solving the diffusion equation:

$$\frac{\mathrm{d}\Sigma}{\mathrm{d}t} = \frac{3}{r}\frac{\partial}{\partial r}\left[r^{1/2}\frac{\partial}{\partial r}(\tilde{\nu}\Sigma r^{1/2})\right] + \dot{\Sigma}_w(r), \quad (3)$$

where $\tilde{\nu}$ is the mean viscosity (integrated along the z-axis), and $\dot{\Sigma}_w(r)$ is the photoevaporation term, taken as in Veras & Armitage (2004). The viscosity is calculated in the framework of the α formalism (Shakura & Sunyaev 1973) after first solving for the vertical structure of the disc (see Alibert et al. 2005c). This calculation also gives us the evolution of the thermodynamic conditions inside the disc, as a function of time and heliocentric distance. These conditions are used, together with information on the composition of the nebula's gas, in order to derive the amount of volatile species trapped inside icy planetesimals. For the model we use here, the α parameter is equal to 2×10^{-3}, and the total evaporation rate is of the order of $10^{-8}\,M_\odot\,yr^{-1}$. At the beginning of the calculation, the gas surface density is given by a power law, $\Sigma \propto r^{-3/2}$, normalized to have $\Sigma = 600\,g\,cm^{-2}$ at the current day position of Jupiter. As stated above, this disc model was used in Alibert et al. (2005b) in order to calculate formation models of Jupiter and Saturn. The resulting thermodynamic conditions are plotted in Fig. 3 for early epochs during the evolution of the solar nebula.

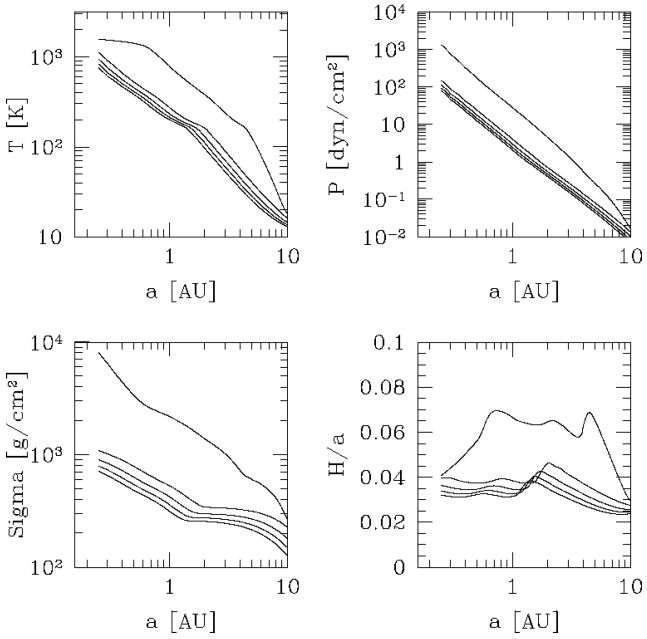

Figure 3. Thermodynamic conditions in our disc model. Top left: mid-plane temperature profile; top right: mid-plane pressure profile; bottom left: surface density profile; bottom right: aspect ratio H/a profile (H is the semithickness and a the heliocentric distance). The epochs shown in the four panels are, from top to bottom, 10^4 yr, 0.5, 1, 1.5 and 2 Myr.

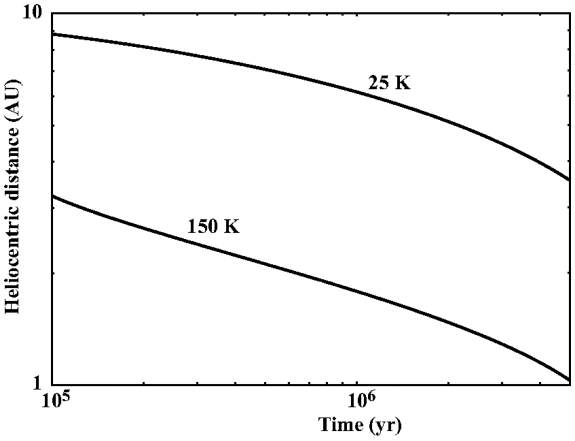

Figure 4. Locations of the 25 K- and 150 K-lines as a function of time for our model of the primitive nebula.

Fig. 4 shows the location of the snowline[6] and the 25 K-line[7] as a function of time. In our calculations, we assume that when a particle

[5] The work of Cyr et al. (1998) is based on the static solar nebula models elaborated by Cassen (1994). In each of these models the position of the condensation front of water (the 'snowline') remains at a constant heliocentric distance. In contrast, evolutionary models cool with time and allow the snowline to migrate closer to the Sun.

[6] The sublimation temperature of water ice is taken as 150 K, and does not depend on pressure in our calculations.

[7] At temperatures lower than ∼25 K, all the main volatile species are presumed to be trapped as clathrate hydrates or in the form of pure condensates in the solar nebula (e.g. Fig. 1).

reaches the snowline (or the 25 K-line), it loses all its volatiles (or loses all the volatile species whose condensation temperatures are lower than or equal to 25 K). This is of course a simplification, and more accurate calculations should take into account the progressive heat diffusion, and the resulting sublimation, within icy particles entering the warmer regions of the early solar nebula. That such low temperatures are reached at small heliocentric distances in the solar nebula can be surprising, given that the equilibrium radiation temperatures are of ∼160 K at 3 au. However, our calculations are justified by the fact that, during the lifetime of the nebula, the Sun's radiation is significantly attenuated, even at distances of a few astronomical unit, due to Rayleigh scattering from molecular hydrogen and dust opacity, in particular if no inner gap is postulated in the disc (Mousis et al. 2007). In these conditions, light becomes extinguished close to the star as a result of the high gas density, while the outer regions play little role in the extinction. For temperatures below 1500 K, the dominant dimming effect in the nebula at wavelengths shorter than a few micrometre is Rayleigh scattering from molecular hydrogen (Mayer & Duschl 2005). This condition is fulfilled for the entire nebula after 10^5 yr, with the temperature beyond 0.6 au already falling below 1000 K at this early stage. Moreover, the mass absorption coefficient has been estimated to be $\sigma_m = 5 \times 10^{-4}$ (cm^2 g^{-1}) in the solar nebula (Mousis et al. 2007). Integrating along the mid-plane radial axis of the model from 0.25 au (the inner edge of the disc), the optical depth at 3 au is initially about $\tau = 18$. It decreases over time to $\tau = 5.3$ after ∼5 Myr of the disc's evolution. As a result, only ∼0.5 per cent of the star's radiation will be available at this distance within the disc at this epoch. We can therefore assume that the disc remains optically thick to solar radiation during at least the first 5 Myr of its evolution. Note also that it has been recently showed that discs with puffed up inner edge could shield part of their outer edge from star light, in agreement with the structure and the overall spectral energy distribution (SED) of protoplanetary discs around Herbig Ae/Be stars (Dullemond & Dominik 2004). This is the case for our solar nebula model which is self-shadowed at heliocentric distances higher than ∼2–3 au (see semithickness over heliocentric distance profile in Fig. 3). Since the Rayleigh scattering, as well as the strong opacity of grains impede the light to go through the upper layers and illuminate the outer parts of the disc, the cooling of the nebula down to low temperatures should follow, even in the formation zone of asteroids.

In our calculations, we have considered particles of various sizes, ranging from 1 cm to 100 m. We assume that they are formed at different locations in the nebula, and at different epochs, in a similar way to MA05. Fig. 5 shows the trajectories of particles of size 1 cm, 10, 30 and 100 m. For particles ranging between a few centimetres and a few metres in size, gas drag is so strong that the trajectories would be represented as vertical lines. The trajectories of the particles are stopped when they cross the iceline. Fig. 5 shows that, due to gas drag, particles with the sizes considered here can drift to the present day location of the main belt. The innermost location of particles that have not suffered any sublimation of ice is therefore given by the location of the snowline at a given time. Similarly, the 25 K-line gives, as a function of time, the innermost location of particles that have not lost any of their volatiles. The situation is more complex for particles massive enough to significantly decouple from the gas, which therefore experience minimal, if any, orbital decay (see last panel n 100-m-size objects – in Fig. 5). Icy material can thus be transported by such medium size particles. If they cross the 25K-line, they would be expected to lose some fraction of their volatile content. However, particles formed even later, after a few Myr of the evolution of the solar nebula, but before it becomes optically thin, do not encounter temperatures higher than 25 K. They can therefore preserve all of their volatile species from vaporization until their capture by forming asteroids.

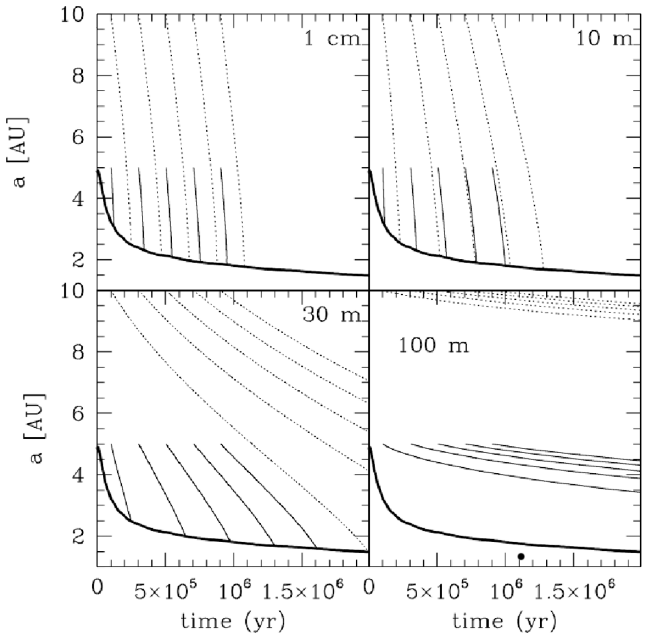

Figure 5. Trajectories of solid particles in the primitive nebula, for different starting location and starting epochs. The initial location of particles is either 5 or 10 au, and the drift starts during the first Myr of the solar nebula evolution. The trajectories are drawn until particles cross the iceline (heavy solid line), from which they are assumed to vaporize. The size of particles is given in each panel, and their density is equal to 1 g cm^{-3}.

On the other hand, even if icy particles may have drifted to heliocentric distances low enough to take part to the formation of the whole main belt without losing a non-negligible fraction of their volatiles, the current distribution of ices that actually exists in asteroids has probably been significantly altered during and/or after their formation. Indeed, more heat was generated during the accretion of asteroids located at low heliocentric distances, as impacts and collision velocities were greater. As a result, vaporization has occurred, thus changing the composition of ices incorporated in inner belt asteroids. Moreover, the equilibrium radiation temperatures reached on the surfaces of main belt asteroids after the dissipation of the nebula can be too high for the long-term stability of water ice, particularly in the case of inner belt asteroids (Jewitt et al. 2007). Indeed, even if potential internal heating from the decay of Al^{26} and other isotopes is not considered, radiation equilibrium may have led to the vaporization of the ice content of the nearer asteroids (semimajor axes of ∼2 au), and melted the ice of mid-range asteroids situated at ∼3 au. However, it will probably not have affected the ice in the interiors of asteroids located further out. Inner and outer asteroids would therefore display no detectable hydratation features either because the ice was vaporized and dissipated, or because the ice never melted and thus did not react with other minerals that would enable its detection (Cyr et al. 1998). On the other hand, mid-range asteroids could be expected to have undergone sufficient melting that chemical alteration of silicates would occur and be detectable (Cyr et al. 1998; Jewitt et al. 2007). Water ice could also be present temporarily on the surface of large hydrated bodies like Ceres, while migrating outwards from subsurface layers or

mantle of the asteroids, and before it sublimates into space (Fanale & Salvail 1989).

These considerations imply that the future detection and identification of the volatile phases in asteroids could give some constraints on the thermodynamic conditions that were present within the solar nebula during their accretion, as well as during the inwards migration of icy planetesimals. For example, assuming a cold accretion for asteroids located in the outer belt and that the only detected volatile species on the surfaces of some of their members are CO_2; H_2S, NH_3 and H_2O, one may deduce that the temperature of the nebula on the migration pathway of icy planetesimals was between ∼60 and 80 K (e.g. Table 4). However, we note that alteration of the volatile phases in asteroids may occur after their formation, as a result of catalytic reactions in their interiors. Indeed, this mechanism has been proposed to explain the current composition of the plumes released by the Saturn's moon Enceladus (Matson et al. 2007) and could occur at early epochs following the accretion of asteroids due to internal heating caused by the decay of ^{26}Al. Hence, the influence of this chemistry within the interior of asteroids may also play a role in the composition of the volatile phases that potentially exist in some members of the main belt.

4 IMPLICATIONS FOR THE POROSITIES OF ASTEROIDS

This section is devoted to a discussion of the determination of the taxonomical types of the asteroids, and their densities. It appears that some of the results in this area, due to their low accuracy, provide poor constraints on the internal structures of the asteroids in question, and it is therefore difficult to infer their composition from these measurements. This is particularly true for the M-type asteroids which often show a puzzlingly high albedo, and a measured bulk density much lower than the densities of their supposed analogue metallic meteorites. This implies that our current knowledge of the physical properties of asteroids is not in contradiction with the idea that some of them may have preserved substantial amounts of the ices accreted during their formation. We then discuss the potential influence that the incorporation of ices in asteroids may have on their resulting densities and porosities.

4.1 Uncertainties in the taxonomical class and densities of asteroids

The computation of porosity necessitates the knowledge of both the bulk density of an asteroid and the bulk density of its constituent material. With the exception of the few 'giant' objects or dwarf planets (Ceres, Pallas and Vesta), the bulk density of asteroids is generally smaller than that which would be expected from the densities of supposed meteorite analogues. The relationship between meteorite analogues and sample densities is, however, not straightforward and can, in some cases, be misleading. This is particularly important for the objects classified as M, P or E-type asteroids in the Tholen classification scheme.

Recently, a classification based on spectral morphology has been proposed by Bus, Vilas & Barucci (2002), where these asteroids are related to class X and subclasses therein. Asteroids within these classes generally display a linear trend in their reflectance curve, and often also have high albedo. In the case of radar observations, some M-type asteroids also showed particularly strong echo signatures, suggesting they are essentially made of metal, just like the M-type meteorites. However, this might not be always the case, and some X-type asteroids could also be closer to primordial D- or P-type objects, and hence have lower densities. In any case, their connection to meteorites is either unknown or unclear (Clark et al. 2003; Hardersen, Gaffey & Abell 2005) and has been under debate during the last decade. M-type asteroids were generally thought to be the remnants of the metallic cores of differentiated asteroids or planetesimals that would have lost their silicate mantle, possibly after a disruptive catastrophic collision. There is still debate about the composition and origin of M- or X-type asteroids (Busarev 1998; Rivkin et al. 2000). Following Lupishko & Belskaya (1990), a purely metallic composition is hard to believe, and E-type chondrites or stony-iron meteorites could be better analogues. Nowadays it appears likely that these classes comprise an assemblage of several possibly unrelated surface types with a featureless spectrum, not all of which are metallic. Indeed, some asteroids previously classified as M-type have shown spectra with the 3 μm signature associated with aqueous alteration which clearly makes this metallic-core hypothesis less viable. Similarly, 21 Lutetia has been classified as an M-type asteroid since its albedo is relatively high, but recent spectroscopic observations suggest it is actually a classical C-type body (Lazzarin et al. 2004).

On the other hand, the bulk density of an asteroid is derived from measurements of its mass and size. Mass determinations obtained as a result of the dynamical perturbations experienced during close encounters are less accurate, particularly when they are based on a single target perturbation (Hilton 2002). One can find large discrepancies when comparing the values obtained by this technique to the one derived from the analysis of a moonlet's orbit. For example, the masses of 22 Kalliope and of 87 Sylvia differ by a factor of 2 between Marchis et al. (2003) and Kochetova (2004), or between the results of Marchis et al. (2005) and Ivantsov (2007), where the latter values should theoretically be the less accurate ones. There are also large discrepancies between different results obtained from the same technique but involving different observations: depending on the authors, the mass of Psyche ranges from $(0.68 \pm 0.14) \times 10^{-11}$ to $(0.87 \pm 0.26) \times 10^{-11}$ or $(1.49 \pm 0.31) \times 10^{-11}$ $M_\odot$ (Lupishko 2006) or even up to $(3.38 \pm 0.28) \times 10^{-11}$ or $(4.0 \pm 1.4) \times 10^{-11}$ $M_\odot$ (Kuzmanoski & Kovačević 2002; Ivantsov 2007), all values that are generally outside the usual statistical 3σ margin. Finally, an error in the size of the body (mainly resulting from the determination of the object's albedo) will introduce a large error in the determination of the bulk density. We find that the revised density of Psyche from the polarimetric albedo of Lupishko (2006), together with the largest value for the mass of Kuzmanoski & Kovačević (2002), would then reach the unrealistic value of $\rho = 13.2\,\mathrm{g\,cm^{-3}}$. None the less it is stressed that the matching between the *IRAS*-based diameters and the sizes measured from resolved asteroids in the main belt is generally good (Cellino et al. 2003; Marchis et al. 2006), in contradiction with the latter disagreement of Lupishko (2006) for this particular M-type asteroid.

It therefore seems that it is difficult to obtain meaningful statistics using the taxonomic M-type class because diversity is still present (the situation is barely improved when one considers Bus et al.'s X-class). It is therefore clear that an average value for the density of the M-type asteroids (e.g. Krasinsky et al. 2002) can be misleading. It would also be difficult to derive knowledge of the internal structure of these bodies since the bulk densities quoted in the literature can often be in error.

4.2 Influence of the volatile content in asteroids on their bulk densities

Considering the delivery scenario detailed in Section 3, the asteroids would have been accreted from a mix of icy solids that formed

initially in the outer solar nebula, and that preserved their volatile content during their inward migration, with heavier and possibly differentiated material produced at smaller heliocentric distances. Such a scenario would not, however, be applicable to the gravitationally re-accumulated aggregates that result from a catastrophic collision (such as rubble-pile asteroids, and possibly binary objects), because their formative collisions would happen at a later stage of the evolution of the Solar system. Nevertheless, ices could still be present in rubble-pile asteroids even after exposure to solar irradiation.

The time-scale for re-accumulation scales as $(G\rho)^{-1/2}$, where G is the gravitational constant and ρ the density of the body, so that the dynamical time-scale for the re-accumulation of the aggregates is – depending on their actual velocity dispersion – of the order of several days (Michel et al. 2001; Durda et al. 2004; Michel, Benz & Richardson 2004; Nesvorný et al. 2006). This corresponds roughly to a few revolutions of the debris (the remaining material would be ejected). At times larger than several weeks, debris are no longer accumulated, but rather dispersed into a dynamical family. The time-scale for re-accumulation after a catastrophic disruption of an asteroid is thus of the order of weeks. On the other hand, the sublimation rate experienced by the debris depends on several conditions: temperature (heliocentric distance), and the presence and thickness of soil and regolith (Chevrier et al. 2007). The sublimation rate for a planar surface of pure ice is proportional to $P_s(M/2\pi RT)^{-1/2}$ in a vacuum (e.g. Novikov & Vagner 1969; Patashnick & Rupprecht 1975; Farmer 1976), where P_s is the saturation vapour pressure at T, M the molecular weight, R the universal gas constant and T the temperature.

Depending on the author, the coefficient factor used to calculate the sublimation rate from this proportionality incorporates different effects (such as the rugosity, presence of other gas, soil shell burying the ice, etc.) and can vary within two orders of magnitude. The evaporation rate is, however, of the order of 1 m year^{-1} at most (Hsieh & Jewitt 2006; Andreas 2007). At 160 K, which is a typical temperature for a moderate albedo body in the main belt, the recession rate of water ice can be as low as a few mm yr^{-1} (Hsieh, Jewitt & Fernández 2004). The sublimation lifetime for kilometre sized bodies is therefore of the order of a few thousand years.

The dynamical time for re-accumulation is therefore much shorter than that for the sublimation of all the ice in collisional debris. As a consequence, one can neglect for our purpose the evaporation of ices during the post-impact re-accumulation phase. We argue that water and other volatiles are not easily revealed, and that such hidden ices will have a significant influence on the internal structure and porosity of the asteroids. Such a scenario was suggested by Veverka et al. (1997) for the asteroid 253 Mathilde, but rejected by the authors in the absence of any alteration feature in the spectra. Similarly, Wilson et al. (1999) consider the case where all volatiles must have been completely lost, thus increasing the porosity, but again only for the altered bodies. In general, the presence of an unrevealed icy fraction will reduce the expected bulk density (the body's average mass-to-volume ratio), regardless of its mass distribution, as would do the presence of voids and cracks, or any other light material such as a regolith. Thus, a low measured density could be explained by voids or cracks in a rubble-pile structure, or a fractured body, or by the presence of light ices, or both, since these hypotheses are not mutually exclusive. In the following discussion, we address the bias introduced by the presence of ices in a simple computation of the macroporosity of an object.

The macroporosity of an asteroid is calculated by the determination of the fraction of empty space within the total volume, which translates to $1 - \rho_b/\rho$ where ρ_b and ρ are the measured bulk density

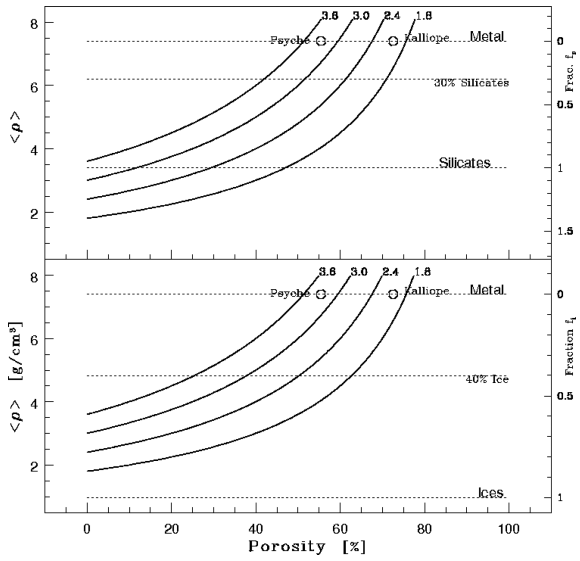

Figure 6. The porosity of asteroids considering a possible volume fraction of ices (f_i) or silicates (f_s) of density $\rho = 0.97$ or 3.4, respectively. The ordinate is the average sample density $\langle\rho\rangle = f_i(\rho_i - \rho) + \rho$. The different curves correspond to various values of measured bulk densities (ρ_b) of asteroids. Upper panel: porosity for M-type asteroids with both metal ($\rho = 7.4$) and silicaceous components. Bottom panel: porosity for M-type asteroids with both metal and ices.

of the asteroid and the assumed sample bulk density, respectively. Following Britt et al. (2002), the (uncompressed) sample density is derived through knowledge of the asteroid's taxonomic type, using values measured in meteoritic analogues, and taking into account microporosities in the meteoritic grain. This macroporosity can now be computed by taking into account a possible volume fraction of ices f_i or silicates $f_s = V_s/(V_s + V_i)$ (where V_s and V_i are the volume of silicates and ices, respectively), so that $f_s + f_i = 1$. This corresponds to an effective sample density $\bar{\rho}_s = f_s(\rho_s - \rho_i) + \rho_i$, and the bulk porosity is now given by

$$\psi = 1 - \frac{\rho_b}{f_i(\rho_i - \rho_s) + \rho_s}, \quad (4)$$

where one finds the limiting values of porosity for $f_i = 0$ and 1.

As can be seen in Fig. 6, the bulk porosity of an object with a significant icy component can remain relatively low, in the fragmented regime of Britt et al. (2002). The corresponding mass fraction is $X_i = (\rho_i/\rho_s)\, f_i/(1 - f_i) \approx [3(1/f_i - 1)]^{-1}$ for typical values of ice and silicates. Thus the value of $X_i = 17$–27 per cent for the water content by mass determined by McCord & Sotin (2005) in the case of Ceres translates to $f_i \approx 40$ per cent in volume. Note that the values shown in the figure are not strictly restricted to water ice. Indeed, the densities of the considered hydrates, clathrate hydrates or pure ices are very close to that of water ice ($\sim$0.9 g cm^{-3}). Nevertheless, if a large fraction of ice must be present in a given body, it is most likely that they would consist of H_2O and CO_2, as shown in Table 5.

Assuming a mass fraction of silicate or ices together with metallic components would lead to a reduction of the mean sample density $\langle\rho\rangle$, and hence the computed bulk porosity. As shown in Fig. 6, the porosity of M-type asteroids 22 Kalliope and 16 Psyche (both X type in the Bus et al. classification) with the adopted updated bulk densities of $\rho = 2.03$ g cm^{-3} (Marchis et al. 2003) and $\rho = 3.3$ g cm^{-3} (Lupishko 2006), respectively, could be reduced by considering a substantial volume fraction of either silicates (olivine, pyroxene) or

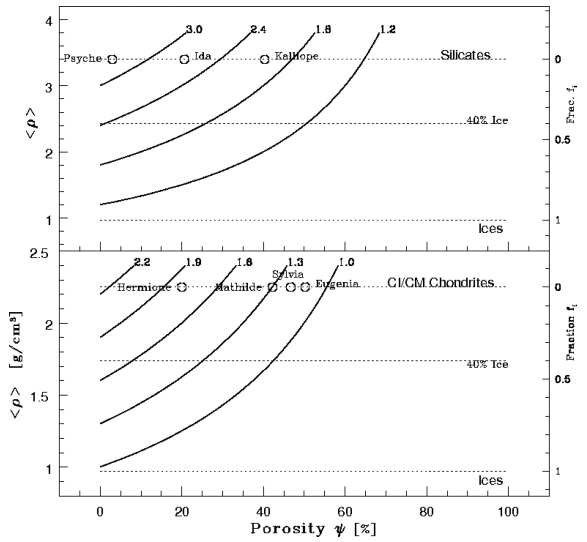

Figure 7. Same as Fig. 6 with the volume fraction of ices (f_i) and silicates ($\rho = 3.4$) or the lightest chondrites ($\rho = 2.2$). Upper panel: porosity for S-type asteroids with some icy fraction (right-hand legend). Bottom panel: porosity of C-type asteroids with ices.

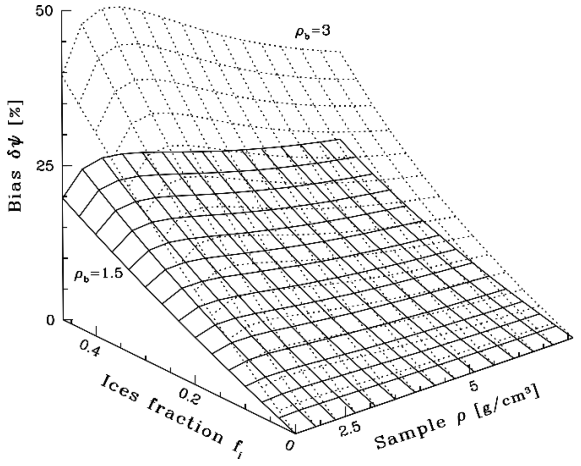

Figure 8. The bias introduced in the computation of the porosity (ψ) by neglecting a possible presence of ices (equation 4). Its resulting value is given as a function of the actual volume fraction of ices (f_i) and the sample density (ρ_b) of the body. It is plotted here for two cases of ρ_b (solid and dotted grid).

ices (water, . . .). In the case of Kalliope, however, only a large mass fraction of silicates or ices could reduce the porosity to a realistic packing for a supposedly post-collisional gravitationally bound granular material (i.e. less than approximately 50 per cent). Psyche is a controversial object because its radar echo is high, which makes a metallic surface plausible. Keeping in mind that the error bars are so large that its density could be in the range (1.7–13.2), it is clear that the lowest values are feasible only if a significant fraction of lighter material is introduced. Moreover, in this latter case, there is no reason to expect a porosity larger than 20–30 per cent, i.e. larger than that assumed for fractured objects. Furthermore, considering that these bodies' main constituent is of a lower density (closer to those of silicates or stony-iron meteorites ∼3.3–4.5), one sees that these could still contain a fraction of the order of 30 per cent ice.

Similarly, as shown in Fig. 7, one sees that for the low density objects like Eugenia, Mathilde and Sylvia and the C-type asteroids in general, introduction of a significant mass fraction of ices would change the computed porosity of these bodies. Note that a composition of 30 per cent water ice and 70 per cent CI/CM-type chondrites in the Cb-type asteroid 253 Mathilde would imply an average porosity of approximately 30 per cent for both constituents, a value which seems plausible; at least for the porosity of the ice. Pushing this exercise further, one can also derive either the density of the other constituents, by assuming a constant ice content and a constant porosity, or inversely, derive the mass- or volume fraction of ices at constant macroporosity and a given heavy element (chondrite, silicate, stony-iron, etc.) density. For instance, the C-type asteroids Mathilde, Eugenia and the X/P-type Sylvia could all have the same density within their heavy constituents, and a porosity of 40 per cent. This would then require them to contain approximately 5, 15 and 45 per cent water ice, respectively.

In conclusion, water and other volatiles could have remained buried inside the main belt asteroids since the formation of the Solar system without being easily detected by remote spectroscopic observations. The presence of such ices will reduce the value of the bulk density of the body that would be expected from its taxonomic type, and, moreover – given the small amounts of compaction inside asteroids – it will additionally decrease the asteroid's macroporosity (Durham, McKinnon & Stern 2005). There would be no a priori preference of this scenario for any asteroidal taxonomic type (hydrated or not), or collisional evolution (given short re-accumulation time-scales). On the other hand the size and mass of the asteroid may play an important role, which is not addressed here. Neglecting the possible presence of such ices can thus increase the error biases on the computation of the porosity, leading to it being systematically overestimated. For small amounts of ice ($f_i \sim 0.2$, see Fig. 8), the error in the porosity is $\delta\psi \sim f_i\,\rho_b(\rho - \rho_i)/[\rho^2(1 + f_i(\rho_i - \rho)/\rho)]$ which yields a bias in the calculated porosity of at least 5 to 15 per cent depending on the actual bulk density of the asteroid (ρ_b), its supposed sample density (ρ) and obviously on the actual volatile component (f_i). In addition, the precision of asteroids bulk densities measurements is increasing with better knowledge of masses and current high-resolution angular measurements for the size (not to mention space probes). As a consequence, the importance of the error or bias discussed here should become more and more important.

5 SUMMARY AND DISCUSSION

In order to explain the presence of hydratation and cometary features in the main belt, we have proposed that asteroids incorporated during their formation icy particles formed in the outer solar nebula. We have then calculated the composition of the ices trapped in these planetesimals formed beyond a heliocentric distance of 5 au in the nebula, in a manner consistent with the formation of Jupiter, by assuming that the gas-phase abundances of all elements, in particular that of oxygen, are solar. As a result, we have found that the ices being formed in the outer solar nebula are composed of a mix of clathrate hydrates, hydrates formed above 50 K, and pure condensates produced at temperatures between ∼20 and ∼50 K. We have noted that, whatever the input parameters adopted in the modelling of the disc, or the formation location considered for icy planetesimals at heliocentric distances beyond 5 au, their composition remains almost constant, provided that the gas-phase abundances are homogeneous in the nebula. We have argued in this work that gas drag is responsible for the inward drift of icy particles formed in the

outer nebula towards the forming main belt. To support this hypothesis, we have showed that, at some epochs of the disc's evolution, some particles produced in the outer nebula may drift to the current position of the main belt without encountering temperature and pressure conditions high enough to vaporize the ices they contain.

The current distribution of ices potentially existing in asteroids has probably been deeply altered after their formation. The effect of solar insolation may have vaporized the ice within nearer asteroids (semimajor axes of $\sim$2 au), melted the ice of mid-range asteroids situated at $\sim$3 au, but should not have affected the ice in asteroids located at greater heliocentric distances. Inner and outer asteroids would therefore display no detectable hydratation features, either because the ice was vaporized and dissipated, or because the ice never melted and thus did not react with the surface minerals to a sufficient extent as to allow detection (Cyr et al. 1998). In this context, we have proposed that, from the detection and identification of initially buried ices revealed by recent impacts on the surfaces of asteroids, it could be possible to infer the thermodynamic conditions that occurred within the solar nebula during the accretion of these bodies, as well as during the inwards migration of the icy planetesimals which they incorporated. However, this statement requires that either no parent body processing or modification took place during and after the formation of asteroids. For example, we have noted that subsequent alteration of the volatile phases in asteroids may occur due to catalytic reactions in their interiors.

We have also investigated the potential influence that the incorporation of ices in asteroids may have on their porosities and densities. In particular, we have showed that the presence of ices can considerably reduce the value of the bulk density of the body, and consequently its macroporosity, that would be expected from a given taxonomic type.

That volatiles were delivered to areas within the ice line is clearly beyond doubt. In addition to the gas-drag mechanism described in this work, it is also likely that a significant amount of volatile material was dynamically driven inwards in the latter stages of planet formation. We still see the tail of this dynamical, chaotic volatile movement today – the comets we observe passing through the inner Solar system are the bearers of ices formed far beyond the snowline, and held in deep freeze since the early days. During the latter stages of planetary migration, the flux of such objects passing through the inner Solar system, and hence encountering the asteroids, was significantly higher. Of particular interest, when one considers veneers of volatile material near the surface of the asteroids, is the Late Heavy Bombardment. In the Nice model, (see e.g. Gomes et al. 2005), vast amounts of volatile-rich material is flung inwards from the outer Solar system approximately 700 Myr after its birth. This event, caused by the resonant destabilization of the outer Solar system, would have coincided with a simultaneous stirring of the asteroid belt, leading to an impact flux upon the Earth containing approximately even proportions of asteroidal and cometary material. It is clear, though, that the Earth would not be the only object to encounter volatiles injected in this way, and the possibility of a late veneer of ice arriving in the asteroid belt is surely something which must be acknowledged in future work. In addition to this aggressive and chaotic injection of material, there is also a gentler mechanism by which volatiles can be driven inwards as a result of planetary migration. As planets migrate, material can be trapped in the locations of mean-motion resonances (MMR), which sweep in front of the planet through its motion. Evidence of material being swept outwards in the resonances of Neptune is clear for all to see – the Plutino family of objects are locked in the 2:3 MMR with the planet, and have an inclination distribution which can tell us a great deal about the distance over which the planet migrated, sweeping them along. Inward migration can have the same effect – the interior resonances of a planet can collect material as it moves inwards, and sweep it along – giving a mechanism by which volatile material can be eased inwards, with the migration of a giant such as Jupiter. Work such as Fogg & Nelson (2006) has shown that such resonant forcing can operate with a reasonable efficiency, even for significantly faster migration than expected in our Solar system, and so the effects of this behaviour should not be ignored in future work.

In spite of the growing pool of evidence pointing towards the existence of water ice in the main belt, its detection on asteroids is a challenging observational problem. Large bodies such as Ceres are suspected to have retained a large amount of water since their formation, perhaps even including an internal liquid ocean, throughout the age of the Solar system (McCord & Sotin 2005). This could particularly be the case if this internal water was originally mixed with some ammonia, in agreement with our composition calculations in Section 2.3, which would have the effect of lowering the melting point of the water (ammonium bearing minerals have been suggested by King et al. 1992 as an alternate explanation for the origin of the 2.07-μm band seen in the spectrum of Ceres). Nevertheless, internal water can only be indirectly probed, either by measuring the hydrostatic shape of the object, as was done in the case of Ceres, or by inferring its density from its size and mass, when they are known or, more evidently, from outgassing activities. The case of Ceres is particularly interesting since, in spite of several possible pieces of evidence which support it being a highly hydrated body, the only report of water detection on the dwarf planet is the observation of OH escaping from its northern pole[8] is still not confirmed. Nevertheless, this detection could be explained in the context of the accumulation of ice during winter on the surface or within the subsurface layer, which would then dissipate during summer, when the surface temperature rises. Similar transient events have been suggested as possible mechanisms to trigger the geyser-like activity taking place near the south pole of Enceladus and reported by Cassini (Porco & Team 2006).

It is interesting to note that, considering the gravity and the dayside temperature of Ceres, any outgassed atmosphere would be rapidly lost. The mean thermal velocity v_0 of H_2O, for instance, would be close to the escape velocity ($v_\infty = 516\,\mathrm{km\,s^{-1}}$). Assuming a subsolar temperature of 215 K (Dotto et al. 2000), v_0 would vary between 450 and 350 $\mathrm{km\,s^{-1}}$ from the subsolar point to a zenith angle of 80°. As a consequence, hydrodynamical escape would occur ($v_{\mathrm{esc}}^2/v_0^2 \leqslant 2$). The photolysis of H_2O by solar extreme ultraviolet (EUV) makes this atmospheric escape even more efficient by giving the photodissociation products OH and H some additional kinetic energy. Considering the short lifetime of H_2O at $\sim$3 au (<9 d), and the fact that the mean thermal velocity of H atoms exceeds v_∞, a tenuous atmosphere of OH is expected if water is outgassed by the asteroid at a sufficient rate. Because of the transient nature of the atmosphere, the loss of water to space is limited by the flux of water from the interior to the surface. At low latitude, where ice is not stable, the continuous flux of water from the interior to space is too low to be detected. Only an accumulation of water ice at high latitude before perihelion, followed by an outgassing of H_2O associated with post-perihelion warming seems to result in an observable column

[8] An OH atmosphere was indeed observed around Ceres after perihelion by A'Hearn & Feldman (1992) by performing *IUE* (*International Ultraviolet Explorer*) long exposure spectra, with column densities of the order of $10^{11}\,\mathrm{cm^{-2}}$.

density of OH. These results were found to be consistent with an earlier work done by Fanale & Salvail (1989), who estimated the mean loss rate of H_2O to be in the range 30–300 g s^{-1}. Even if one assumes that the atmospheric loss observed by A'Hearn & Feldman (1992) occurs continuously at the same rate and at all latitudes (which is obviously wrong as this maximum loss requires high latitudes and post-perihelion conditions), the water loss remains below 4 kg s^{-1}, which, integrated over 4.5 Gyr, corresponds to only 0.07 per cent of the mass of Ceres. If the loss rate of H_2O in Ceres remained constant throughout its thermal history, the initial water reservoir is thus likely to be integrally preserved. Moreover, since the other volatile species are expected to be trapped as hydrates, clathrate hydrates and pure condensates in this reservoir, we can conclude that they have also been preserved from outgassing throughout the thermal history of the asteroid.

Ceres being the largest and, due to its size, probably the wettest main belt asteroid, it is an ideal target for carrying out observations aiming at constraining its water regime. The experiment searching for water being vaporized within the polar regions of Ceres should be repeated with the state-of-the-art instrumentation available today on large telescopes. Such detection would confirm unambiguously the presence of a large amount of water near the surface of Ceres. Direct observation of water ice, or of the effects of hydration, on the surface of Ceres can also be attempted for lower latitudes on the asteroid using a combination of high angular resolution and spectroscopic instruments permitting the full resolution of its surface to the 30–40 km level. Because of its low spectral resolution, imaging of the surface of Ceres, even when it is spatially resolved using *HST* or adaptive optics, is not sensitive to the presence of ice, while the detection of such is within the reach of low resolution spectroscopic observations (e.g. the detection of absorption features in the 1.0–3.5 μm region). A spatially resolved spectroscopic mapping of the surface of Ceres in the near-infrared (IR) can be done with today's ground-based telescopes and would permit the mapping of the strength of the 3-μm band, and allow the search for regions on the surface where interstitial water ice, or hydration features could be present, for instance at the location of cracks within the surface of Ceres, or the locations of deep impact craters. Indeed, recent *HST* (Thomas et al. 2005) and adaptive optics (Carry et al. 2007) imaging observations of Ceres revealed the presence of large impact craters across its surface which have likely disrupted the outer crust of the asteroid enough to directly expose the subsurface mantle of wetter material. Finally, a spectroscopic study of the surface of Ceres, in order to search for the spectral signature of water and maybe those of other volatiles, should not be limited to one wavelength region (although the near-IR range offers many diagnostic bands) but should, instead, encompass a wider range, from the near-UV to IR wavelengths, in order to improve the identification of the chemicals species responsible for these spectral features.

Finally, the NASA Discovery mission *Dawn*, which has been launched in 2007 September and whose arrival at Ceres is scheduled for 2015, will certainly bring new constraints on the presence of volatiles in the main belt. In particular, the *Dawn* mapping spectrometer (MS) covers the spectral range from the near-UV (0.25 μm) through the near-IR (5 μm) and has moderate to high spectral resolution and imaging capabilities (Russell et al. 2004). These characteristics make it an appropriate instrument for determining the asteroid's global surface composition. Near-IR mapping of the surface of Ceres at small spatial scales will be very sensitive to volatile concentrations and may reveal ice spots on fresh impact-crater ridges. Moreover, the gravitation investigation of Ceres will allow the determination of its gravity field up to the 12th harmonic degree (Russell et al. 2004). Such a measurement will enable the shape and gravity models to characterize crustal and mantle density variations and, consequently, the amount of volatiles trapped therein.

ACKNOWLEDGMENTS

This work was supported in part by the Swiss National Science Foundation. JH gratefully acknowledges the financial support provided by PPARC. We thank Jean-Marc Petit and Jeffrey Cuzzi for helpful remarks. Many thanks to the anonymous referee whose useful comments invited us to strengthen our manuscript.

REFERENCES

A'Hearn M. F., Feldman P. D., 1992, Icarus, 98, 54
Alibert Y., Mordasini C., Benz W., 2004, A&A, 417, L25
Alibert Y., Mousis O., Benz W., 2005a, ApJ, 622, L145
Alibert Y., Mousis O., Mordasini C., Benz W., 2005b, ApJ, 626, L57
Alibert Y., Mordasini C., Benz W., Winisdoerffer C., 2005c, A&A, 434, 343
Allamandola L. J., Bernstein M. P., Sandford S. A., Walker R. L., 1999, Space Sci. Rev., 90, 219
Andreas E. L., 2007, Icarus, 186, 24
Britt D. T., Yeomans D., Housen K., Consolmagno G., 2002, Asteroids III, 485
Bus S. J., Vilas F., Barucci M. A., 2002, Asteroids III, 169
Busarev V. V., 1998, Icarus, 131, 32
Carry B., Dumas C., Fulchignoni M., Merline W., Berthier J., Hestroffer D., Fusco T., Tamblyn P. 2007, A&A, submitted
Cassen P., 1994, Icarus, 112, 405
Cellino A., Diolaiti E., Ragazzoni R., Hestroffer D., Tanga P., Ghedina A., 2003, Icarus, 162, 278
Chevrier V., Sears D. W. G., Chittenden J. D., Roe L. A., Ulrich R., Bryson K., Billingsley L., Hanley J., 2007, Geophys. Res. Lett., 34, 02223
Chick K. M., Cassen P., 1997, ApJ, 477, 398
Ciesla F. J., Cuzzi J. N., 2006, Icarus, 181, 178
Clark B. E., Rivkin A. S., Bus S. J., Sanders J., 2003, Div. Planet. Sci. Meet., 35, 955
Clayton R. N., Mayeda T. K., 1996, Geochim. Cosmochim. Acta, 60, 1999
Cuzzi J. N., Ciesla F. J., Petaev M. I., Krot A. N., Scott E. R. D., Weidenschilling S. J., 2005, Chondrites and the Protoplanetary Disk, 341, 732
Cyr K. E., Sears W. D., Lunine J. I., 1998, Icarus, 135, 537
Dotto E. et al., 2000, A&A, 358, 1133
Dullemond C. P., Dominik C., 2004, A&A, 417, 159
Durda D. D., Bottke W. F., Enke B. L., Merline W. J., Asphaug E., Richardson D. C., Leinhardt Z. M., 2004, Icarus, 167, 382
Durham W. B., McKinnon W. B., Stern L. A., 2005, Geophys. Res. Lett., 32, 18202
Fanale F. P., Salvail J. R., 1989, Icarus, 82, 97
Farmer C. B., 1976, Icarus, 28, 279
Fegley B. J., 2000, Space Sci. Rev., 92, 177
Fogg M. J., Nelson R. P., 2006, Int. J. Astrobiol., 5, 199
Gautier D., Hersant F., Mousis O., Lunine J. I., 2001a, ApJ, 550, L227
Gautier D., Hersant F., Mousis O., Lunine J. I., 2001b, ApJ, 559, L183
Gibb E. L., Whittet D. C. B., Boogert A. C. A., Tielens A. G. G. M., 2004, ApJS, 151, 35
Gomes R., Levison H. F., Tsiganis K., Morbidelli A., 2005, Nat, 435, 466
Hardersen P. S., Gaffey M. J., Abell P. A., 2005, Icarus, 175, 141
Hersant F., Gautier D., Huré J.-M., 2001, ApJ, 554, 391
Hersant F., Gautier D., Lunine J. I., 2004, Planet. Space Sci., 52, 623
Hilton J. L., 2002, Asteroids III, 103
Hsieh H. H., Jewitt D., 2006, Sci, 312, 561
Hsieh H. H., Jewitt D. C., Fernández Y. R., 2004, AJ, 127, 2997
Irvine W. M., Knacke R. F., 1989, Origin Evol. Planet. Satell. Atmosphere, 3

Ivantsov A., 2007, Planet. Space Sci., submitted
Jewitt D., Chizmadia L., Grimm R., Prialnik D., 2007, Protostars and Planets V, 863
King T. V. V., Clark R. N., Calvin W. M., Sherman D. M., Brown R. H., 1992, Sci, 255, 1551
Kochetova O. M., 2004, Solar Syst. Res., 38, 66
Kouchi A., Yamamoto T., Kozasa T., Kuroda T., Greenberg J. M., 1994, A&A, 290, 1009
Krasinsky G. A., Pitjeva E. V., Vasilyev M. V., Yagudina E. I., 2002, Icarus, 158, 98
Kress M. E., Tielens A. G. G. M., 2001, Meteorit. Planet. Sci., 36, 75
Kuzmanoski M., Kovačević A., 2002, A&A, 395, L17
Lazzarin M., Marchi S., Magrin S., Barbieri C., 2004, A&A, 425, L25
Lebofsky L. A., Feierberg M. A., Tokunaga A. T., Larson H. P., Johnson J. R., 1981, Icarus, 48, 453
Lewis J. S., Prinn R. G., 1980, ApJ, 238, 357
Lide D. R., 2002, CRC Handbook of Chemistry and Physics: a ready-reference book of chemical and physical data. CRC Press
Lodders K., 2003, ApJ, 591, 1220
Lunine J. I., Stevenson D. J., 1985, ApJS, 58, 493
Lupishko D. F., 2006, Solar Syst. Res., 40, 214
Lupishko D. F., Belskaya I. N., 1990, Asteroids, Comets, Meteors III, 129
McCord T. B., Sotin C., 2005, J. Geophys. Res., 110, 5009
Marchis F., Descamps P., Hestroffer D., Berthier J., Vachier F., Boccaletti A., de Pater I., Gavel D., 2003, Icarus, 165, 112
Marchis F., Descamps P., Hestroffer D., Berthier J., 2005, Nat, 436, 822
Marchis F., Kaasalainen M., Hom E. F. Y., Berthier J., Enriquez J., Hestroffer D., Le Mignant D., de Pater I., 2006, Icarus, 185, 39
Matson D. L., Castillo J. C., Lunine J., Johnson T. V., 2007, Icarus, 187, 569
Mayer M., Duschl W. J., 2005, MNRAS, 358, 614
Michel P., Benz W., Tanga P., Richardson D. C., 2001, Sci, 294, 1696
Michel P., Benz W., Richardson D. C., 2004, Planet. Space Sci., 52, 1109
Mousis O., Alibert Y., 2005, MNRAS, 358, 188 (MA05)
Mousis O., Gautier D., 2004, Planet. Space Sci., 52, 361
Mousis O., Marboeuf U., 2006, Div. Planet. Sci. Meet., 38, 13.14
Mousis O., Gautier D., Bockelée-Morvan D., Robert F., Dubrulle B., Drouart A., 2000, Icarus, 148, 513
Mousis O., Gautier D., Bockelée-Morvan D., 2002, Icarus, 156, 162
Mousis O., Petit J.-M., Wurm G., Krauss O., Alibert Y., Horner J., 2007, A&A, 466, L9
Nesvorný D., Enke B. L., Bottke W. F., Durda D. D., Asphaug E., Richardson D. C., 2006, Icarus, 183, 296
Novikov P. A., Vagner E. A., 1969, J. Eng. Phys. Thermophys., 17, 1377
Owen T., Mahaffy P., Niemann H. B., Atreya S., Donahue T., Bar-Nun A., de Pater I., 1999, Nat, 402, 269
Pasek M. A., Milsom J. A., Ciesla F. J., Lauretta D. S., Sharp C. M., Lunine J. I., 2005, Icarus, 175, 1
Patashnick H., Rupprecht G., 1975, ApJ, 197, L79
Porco C., Team C., 2006, Am. Geophys. Union Fall Meet., 1
Rivkin A. S., Howell E. S., Lebofsky L. A., Clark B. E., Britt D. T., 2000, Icarus, 145, 351
Russell C. T. et al., 2004, Planet. Space Sci., 52, 465
Sekine Y., Sugita S., Shido T., Yamamoto T., Iwasawa Y., Kadono T., Matsui T., 2005, Icarus, 178, 154
Shakura N. I., Sunyaev R. A., 1973, A&A, 24, 337
Supulver K. D., Lin D. N. C., 2000, Icarus, 146, 525
Thomas P. C., Parker J. W., McFadden L. A., Russell C. T., Stern S. A., Sykes M. V., Young E. F., 2005, Nat, 437, 224
Veras D., Armitage P. J., 2004, MNRAS, 347, 613
Vernazza P., Mothé-Diniz T., Barucci M. A., Birlan M., Carvano J. M., Strazzulla G., Fulchignoni M., Migliorini A., 2005, A&A, 436, 1113
Veverka J. et al., 1997, Sci, 278, 2109
Weidenschilling S. J., 1977, MNRAS, 180, 57
Wilson L., Keil K., Browning L. B., Krot A. N., Bourcier W., 1999, Meteorit. Planet. Sci., 34, 479

This paper has been typeset from a TEX/LATEX file prepared by the author.